Scripta Materialia xxx (2017) xxx-xxx

Contents lists available at ScienceDirect

Scripta Materialia

journal homepage: www.elsevier.com

Transmission electron microscopy on as–deposited and freestanding single crystalline $Fe_{70}Pd_{30}$ ferromagnetic shape memory alloy thin film

A. Landgraf[a, *], A. Lotnyk[a], S.G. Mayr[a, b]

[a] Leibniz-Institute of Surface Modification, Permoserstr. 15, Leipzig 04318, Germany
[b] Division of Surface Physics, Faculty of Physics and Earth Sciences, Universität Leipzig Linnéstr. 5, Leipzig 04103, Germany

ARTICLE INFO

Article history:
Received 13 February 2017
Received in revised form 6 April 2017
Accepted 13 April 2017
Available online xxx

Keywords:
Shape memory effect
Martensitic phase transition
Twin variants

ABSTRACT

Within this transmission electron microscopy study, we explore the atomic structure of Fe-Pd thin films with and without supporting single crystalline (001) MgO substrate. We observe a phase structural transition depending strongly on spatial limited stresses. While around the film-substrate interface edge dislocations form to minimize stresses due to the lattice misfit between MgO and Fe-Pd, preferring the face-centered cubic phase, upper sample regions show twinning structures with the face- and body-centered tetragonal phase, respectively. In freestanding films, bct and bcc phases are observed. Compared to unprocessed lift-off films, no hierarchical structure was existent anymore, based on changed stress distributions.

In recent years, much research has been performed on ferromagnetic shape memory materials and first applications have been established – mostly based on Ni-Mn-Ga [1]. Compared to this alloy, $Fe_{70}Pd_{30}$ is still a less investigated material, although it constitutes very interesting properties, e.g. its biocompatibility makes it a promising candidate for medical applications [2]. Due to reorientation of variants in the martensitic phase, this material can exhibit theoretical strains up to 5% based on its crystallographic properties, controllable by an external magnetic field at constant temperatures. However, prerequisite to reach maximum magnetically induced strains is a single crystal of the face-centered tetragonal (fct) martensitic phase, providing high twin boundary mobility and strong magnetocrystalline anisotropy. So far, sufficiently defect-free single crystalline thin films in the fct phase have only been synthesized by ion irradiation [3] and electron beam evaporation [4,5]. The first method requires an implanter or accelerator operating with high energy ions, as low energy ions only implement in the existing structure, but high energy ions cause defects which lead to the desired phase transformation. This yields a high amount of costs and hinders a possible establishment for future industrial usage as microscale actuator material. As for the second, there has not been any nanostructural analysis of these films, but will be provided within this study, based on preliminary TEM investigations of this material system in the fcc phase by L. Kühnemund et al. [6].

The examined films of Fe-Pd with a thickness of 500 nm were prepared by molecular beam epitaxy (MBE) from two independent rate–controlled electron beam evaporators onto MgO (001) single crystals. To obtain films in the martensitic phase a total deposition rate of approximately 0.15 nm/s, substrate temperatures of 900°C and ultra high vacuum conditions (base pressure lower than 10^{-9} mbar) have been chosen - as described in detail before [6]. While cooling down to room temperature, the films traverse the austenite ⇒ martensite transition located – depending on detailed composition and preparation conditions – slightly above room temperature [7]. By dissolving the MgO substrate in a sodium bicarbonate solution [4], one film was released from the substrate afterwards. The samples have been analysed regarding their phase appearance by means of X-ray diffraction, using a Seifert XRD 3003 PTS with Cu K_α radiation in Θ/2 Θ geometry.

For scanning transmission electron microscope (STEM) examination, lamella were cut out of the samples with the AURIGA 3912 Cross Beam (SEM-FIB) Workstation from Carl Zeiss Microscopy GmbH with 30 keV Ga^+-ions. For further reduction of the sample thickness, the lamellae were treated with low energy Ar ions in a Fischione NanoMill system [8] and afterwards examined with an aberration-corrected STEM with a high-angle annular dark field (HAADF) detector, utilizing a Titan G2 60-300 microscope (FEI) at an accelerating voltage of 300 keV. The freestanding film has been glued on a thermally oxidized Si wafer before further lamella preparation to ensure a thin, but stable lamella during TEM examination.

Fig. 1a) shows a STEM micrograph of the cross-section of a Fe-Pd thin film deposited on MgO substrate. Pronounced diagonal lines mark boundaries between differently orientated martensitic variants. While the upper part of the film exhibits a quite regular stripe pattern, the lower part includes unpatterned regions as well. The twin variant orientation shown here is consistent with the FIB cuts reported earlier [9]. Twin boundaries are aligned under 45° to the sample surface (corresponding to the $(101)_{Austenite}$ plane). They either ex-

* Corresponding author.
Email addresses: correspondence@landgraf.se (A. Landgraf); stefan.mayr@iom-leipzig.de (S.G. Mayr)

http://dx.doi.org/10.1016/j.scriptamat.2017.04.022
1359-6462/

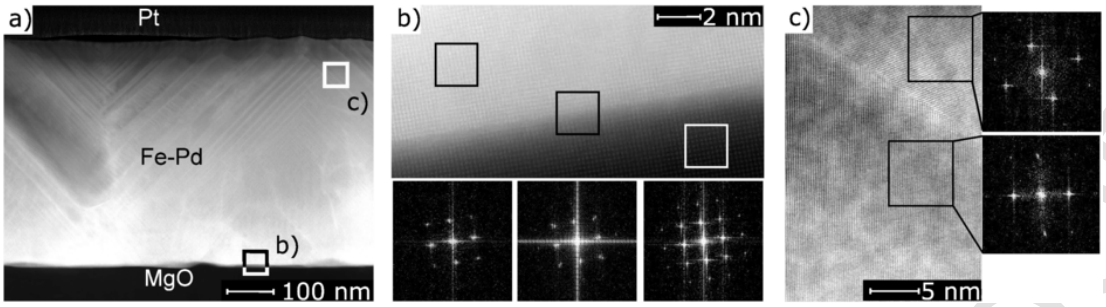

Fig. 1. a) STEM-HAADF image of a 500nm thick Fe-Pd layer on single crystalline MgO substrate with a Pt protective layer on top. Diagonal lines in the Fe-Pd film indicate twin boundaries between crystals of different orientation. The square marked regions were further analysed to examine their crystallographic structure via Fast Fourier Transformation: b) HRSTEM-HAADF image of the interface region between MgO and Fe-Pd. c) HRSTEM-HAADF image of two domains with different orientations in a Fe-Pd thin film.

tend until the MgO or twin boundaries aligned under +45° and −45° to the sample surface join each other, as can be seen in the upper left part of Fig. 1a). Similar to evaporated films in the fcc phase [6], the examined film shows epitaxial growth with a cube-on-cube orientation relationship to the underlaying MgO substrate, confirmed by Fast Fourier Transformation (FFT) of the interface region (see Fig. 1b)). The Fe-Pd lattice spacings in this region were determined to be 0.196 nm and 0.185 nm, corresponding to reported bulk values for the fct phase [10]. Double peak structures (double satellites of main reflections) shown in the FFT image of the pure MgO substrate can be traced back to mechanical vibrations due to the resonance frequencies of the turbomolecular pump, used to assure the vacuum in the TEM [11]. Taking a closer look into the atomic structure of the upper part Fe-Pd-thin film, different twinning variants with an quite sharp twin boundary in between can be found. Analyzing the structure via FFT, as shown in Fig. 1c), lattice spacings of 0.21 nm and 0.15 nm can be determined. Calculating the ratio between these values points to bct structure.

As MgO as substrate material has a larger lattice constant of 0.21 nm compared to the evaporated Fe-Pd thin film, the fct cells will align with both of their long *a* axes in-plane. The remaining misfit still amounts to 9%. To decrease stresses due to this misfit edge dislocations are formed, as marked in Fig. 2a) and previously stated in [6]. The defect density in the interface region has been estimated as illustrated in Fig. 2b) and c). The distance between single dislocations amounts in average to 1.68 nm. Assuming a homogeneous defect distribution as given in part of the high-resolution STEM (HRSTEM) micrograph, a defect density of 3.54×10^{13} cm $^{-2}$ can be calculated.

In general, the formation of the martensitic microstructure is a result of a stress minimization of geometrical constraints. These constraints have already been built up in the austenitic phase due to the substrate attachment and a reduction by arranging different twin domains is enabled during the phase transformation to a martensitic phase[12].

The change in martensitic phase itself with increasing sample depth can be explained quite well by performing STEM- EDX (Energy-dispersive X-ray spectroscopy). Close to the sample surface a composition of $Fe_{75}Pd_{25}$ is measured, close to the MgO substrate the composition approaches $Fe_{73}Pd_{27}$. While the first indicates the appearance of the bct phase, a lower percentage of Iron promotes the fcc and fct phases [10].

Additionally, in another region with pronounced domain structure, this film has been analyzed by Nanobeam Electron Diffraction (NBD). In Fig. 3 different phenomena can be observed: twinned areas (e.g. c and i), which are mainly located in the upper film part, reveal fct double peak structures in the diffraction pattern. In subfigure d lattice constants of 0.186 and 0.188 have been measured, correlating

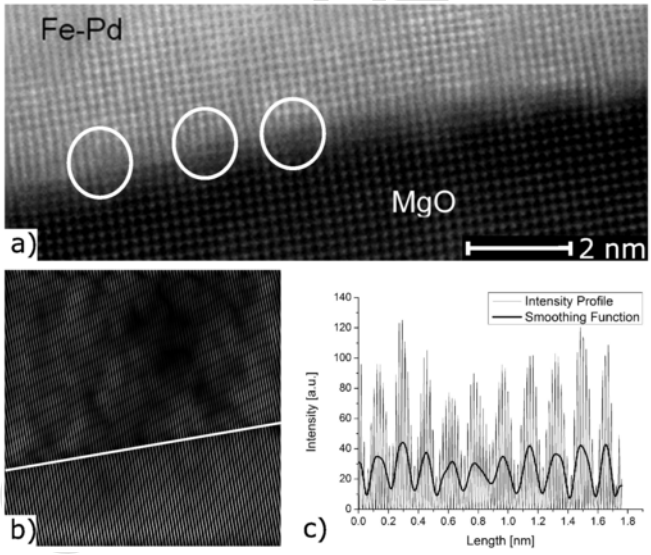

Fig. 2. a) HRSTEM-HAADF micrograph of interface between MgO and Fe-Pd. Edge dislocations are marked with circles. b) FFT Filtered micrograph and c) intensity profile along interface area before and after performing an FFT smoothing function for a better visibility of the edge dislocations.

with the fct-Phase ($(c/a)_{fct} = 0.999...0.94$). Closer to the sample surface in a range of 190 up to around 410 nm, also regions with both - fct (subimage l: $c/a = 0.184/0.19 = 0.968$) and bct (subimage c: $c/a = 0.174/0.194 = 0.897$) structure - can be found. The bct value is not in accordance with literature ($c/a = 0.72$). This indicates, that this region might have not yet completely transformed from fct to bct. As first-principles calculations suggest, only perfect atom positions favour the fct phase [13]. Especially at the interface region between substrate and thin film lattice defects occur. So an increased bct phase can be expected there, whereas in upper regions the number of defects can decrease due to lesser substrate constraints. Furthermore, the transformation from fcc to bcc following the Nishiyama-Wassermann-Path is related with a shear movement [3]. This could lead to a cell orientation which is not optimally suited for lattice constant determination via NBD. In contrast, for unstructured areas close to the substrate like d, k and l only one crystal orientation is noticeable. The STEM image resembles a “tweed” structure, as already observed in polycrystalline fcc Fe-Pd [14]. Close to the MgO substrate double peak structures appear again. While one of these peak constellations can be related with the MgO-substrate itself, the other peak constellation indicates a region with fcc structure.

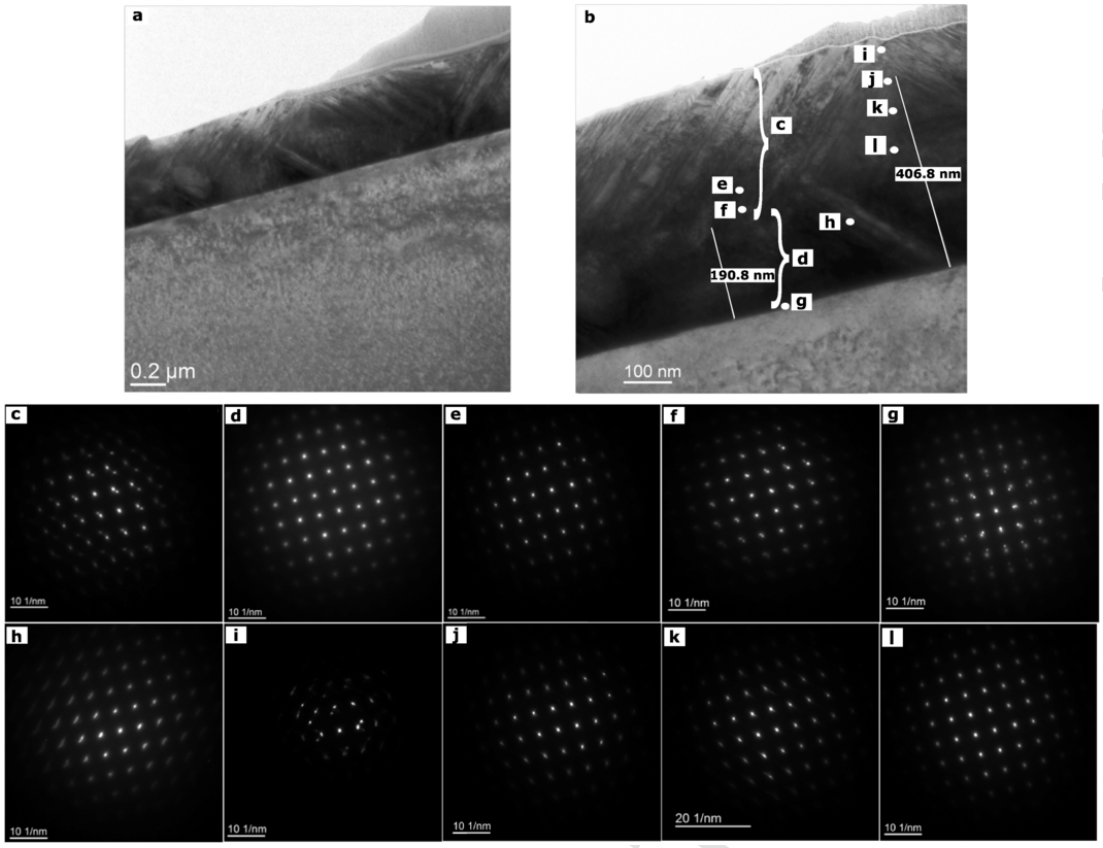

Fig. 3. a) Complete STEM image of the lamella (Fe-Pd on MgO) and b) enlarged image with markings of regions, analysed in detail with Nanobeam Electron Diffraction, shown below the STEM image (c–l). The diffraction pattern indicates a fcc to bct transition starting from the MgO substrate up to the sample surface.

By applying a lift-off procedure, freestanding Fe-Pd thin films with an hierarchical structure are obtained, as reported before [9]. To gain new insight in the atomic structure of elevated and lower microvariants, cross-sections along and perpendicular to these variants are cut and examined with STEM. Surprisingly, micrographs of both cross-sections (not shown here) resemble the STEM image of an as-deposited sample, which was only expected for cross-sections cut along a microvariant. They only differ slightly in the periodicity Λ of their twin zig-zag-pattern. While for freestanding films it amounts to $\Lambda_{freestanding} = 750$ nm, it is $\Lambda_{as\text{-}deposited} = 1000$ nm for as-deposited films. These values are located in the same range as the size of microtwins in freestanding films, which varies between 700 and 1000 nm. In contrast to as-deposited films, freestanding films have no constraints by an attached substrate anymore and therefore form hierarchical structures to reduce shear stress fields in the sample [9,15]. Cutting a lamella perpendicular to the microvariant the alternating sections of twin variant orientation of the corresponding microtwin are changing to a simple zig-zag-pattern (see Fig. 4). As the lamella is much thinner than the film, it is not necessary anymore to keep the structure of the freestanding film, but energetically more favourable

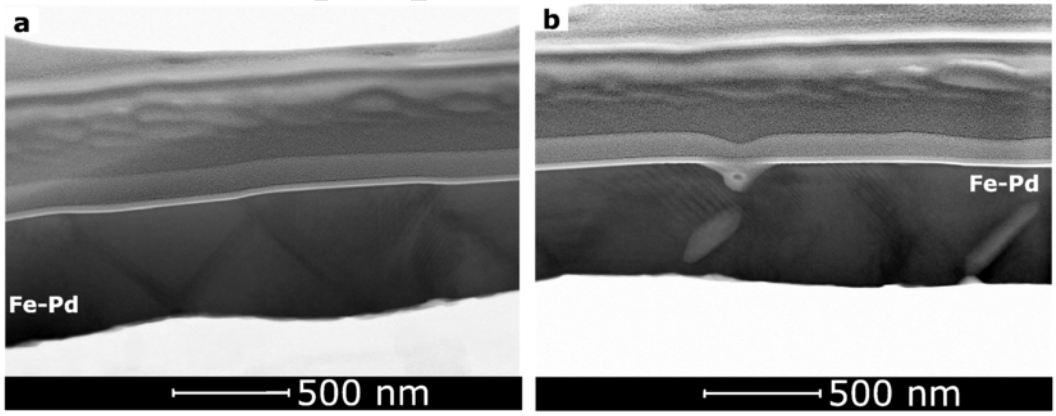

Fig. 4. BF-STEM images of the lamella cut out of a freestanding thin film along a microvariant: a) The Fe-Pd film shows a zig-zag-pattern, which corresponds to the orientation of twin boundaries in the thin film. b) No pronounced zig-zag-pattern, but parallel lines under −45° with respect to the substrate surface.

to form twinning structures of a lower order as the stresses are already reduced by decreasing the thickness of the specimen due to FIB cut and further milling. Here, the bct as well as bcc phase could be observed.

In summary, we achieved an extensive understanding of the phase constitution of Fe-Pd thin films. A strong dependence on local stresses could be found: Close to the MgO substrate a regular arrangement of edge dislocations appears to minimize stress gradients due to the lattice misfit between MgO and Fe-Pd. Here, almost no twin structures can be found. In contrast the upper film part, starting from the sample surface is characterized by pronounced twin structures. Following the thin film from the MgO Fe-Pd interface to the film surface, a subsequent phasetransition from fcc to fct to bct is observed. In lamellas of freestanding thin films only one microvariant orientation showing the bcc and bct phases could be observed due to the changed stress distribution compared to unprocessed films.

Acknowledgements

The authors acknowledge A. Mill for lamella preparation and Prof. B. Rauschenbach for general support. This work is funded by the German Science Foundation (DFG), Project MSMPUMP and was partially performed within the Leipzig Graduate School of Natural Sciences (BuildMoNa).

References

[1] K. Ullakko, J.K. Huang, C. Kantner, R.C. O'Handley, V.V. Kokorin, Appl. Phys. Lett. 69 (13) (1996) 1966.
[2] Y. Ma, M. Zink, S.G. Mayr, App. Phys. Lett. 96 (21) (2010) 213703.
[3] A. Arabi-Hashemi, S.G. Mayr, Phys. Rev. Lett. 109 (2012) 195704.
[4] T. Edler, S.G. Mayr, Adv. Mater. 22 (2010) 4969, http://dx.doi.org/10.1002/adma.201002183.
[5] Y. Ma, A. Setzer, J.W. Gerlach, F. Frost, P. Esquinazi, S.G. Mayr, Adv. Funct. Mater. 22 (2012) 2529, http://dx.doi.org/10.1002/adfm.201103021.
[6] L. Kühnemund, T. Edler, I. Kock, M. Seibt, S.G. Mayr, New J. Phys. 11 (2009) 113054, http://dx.doi.org/10.1088/1367-2630/11/11/113054.
[7] T. Edler, S. Hamann, A. Ludwig, S.G. Mayr, Scr. Mater. 64 (2011) 89, http://dx.doi.org/10.1016/j.scriptamat.2010.09.013.
[8] A. Lotnyk, D. Poppitz, U. Ross, J. Gerlach, F. Frost, S. Bernütz, E. Thelander, B. Rauschenbach, Microelectron. Reliab. 55 (9) (2015) 2119–2125.
[9] A. Landgraf, A.M. Jakob, Y. Ma, S.G. Mayr, STAM 14 (4) (2013) 045003.
[10] J. Cui, T.W. Shield, R.D. James, Acta Mater. 52 (2004) 35, http://dx.doi.org/10.1016/j.actamat.2003.08.024.
[11] T. Kawasaki, Y. Kimura, Y. Takai, R. Shimizu, J. Electron Microsc. 50 (5) (2001) 413–416, http://dx.doi.org/10.1093/jmicro/50.5.413.
[12] S. Kaufmann, R. Niemann, T. Thersleff, U.K. Rößler, O. Heczko, J. Buschbeck, B. Holzapfel, L. Schultz, S. Fähler, New J. Phys. 13 (5) (2011) 053029.
[13] M.E. Gruner, P. Entel, Phys. Rev. B 83 (2011) 214415.
[14] M. Foos, C. Frantz, M. Gantois, J. Phys. Colloq. 43 (C4) (1982) C4–389.
[15] A.L. Roytburd, Phase Transit. 45 (1) (1993) 1–34.